Annals of human genetics

Short Communication

doi: 10.1111/ahg.12134

Charcot-Marie-Tooth Disease Type 4H Resulting from Compound Heterozygous Mutations in *FGD4* from Nonconsanguineous Korean Families

Young Se Hyun[1,†], Jinho Lee[2,†], Hye Jin Kim[1], Young Bin Hong[2], Heasoo Koo[3], Alec S.T. Smith[4], Deok-Ho Kim[4], Byung-Ok Choi[2,5*] and Ki Wha Chung[1*]

[1]*Department of Biological Sciences, Kongju National University, Gongju, Korea*
[2]*Department of Neurology, Sungkyunkwan University School of Medicine, Seoul, Korea*
[3]*Department of Pathology, Ewha Womans University School of Medicine, Seoul, Korea*
[4]*Department of Bioengineering, University of Washington, WA, USA*
[5]*Neuroscience Center, Samsung Medical Center, Seoul, Korea*

Summary

Charcot-Marie-Tooth disease type 4H (CMT4H) is an autosomal recessive demyelinating subtype of peripheral enuropathies caused by mutations in the *FGD4* gene. Most CMT4H patients are in consanguineous Mediterranean families characterized by early onset and slow progression. We identified two CMT4H patients from a Korean CMT cohort, and performed a detailed genetic and clinical analysis in both cases. Both patients from nonconsanguineous families showed characteristic clinical manifestations of CMT4H including early onset, scoliosis, areflexia, and slow disease progression. Exome sequencing revealed novel compound heterozygous mutations in *FGD4* as the underlying cause in both families (p.Arg468Gln and c.1512-2A>C in FC73, p.Met345Thr and c.2043+1G>A (p.Trp663Trpfs*30) in FC646). The missense mutations were located in highly conserved RhoGEF and PH domains which were predicted to be pathogenic in nature by *in silico* modeling. The CMT4H occurrence frequency was calculated to 0.7% in the Korean demyelinating CMT patients. This study is the first report of CMT4H in Korea. *FGD4* assay could be considered as a means of molecular diagnosis for sporadic cases of demyelinating CMT with slow progression.

Keywords: Charcot-Marie-Tooth disease type 4H (CMT4H), compound heterozygous mutations, exome sequencing, *FGD4*, Korean, peripheral neuropathy

Introduction

Charcot-Marie-Tooth disease (CMT) is a group of genetically and clinically heterogeneous peripheral neuropathies with an approximate frequency of 1/2500 births (Pareyson & Marchesi, 2009). CMT is characterized by progressive degeneration of the distal muscles and loss of sensory function. To date, mutations in more than 70 genes have been reported as underlying causes of CMT (Rossor et al., 2013). CMT occasionally exhibits nonstrict genotype-phenotype correlations: defects in different genes can cause similar phenotypes and conversely, defects in the same gene can cause different phenotypes (Kleopa et al., 2004; Nakhro, Park, Choi et al., 2013). CMT is usually classified as either demyelinating neuropathy (CMT1), with median motor nerve conduction velocity (MNCV) of <38 m/s, or axonal neuropathy (CMT2) with MNCV ≥38 m/s (Harding & Thomas, 1980). In Western Europe, the United States, and Japan, autosomal dominant forms of CMT are by far the most frequent. However, in countries that have a high prevalence of consanguineous marriages, such as those of the Mediterranean basin, autosomal recessive inheritance may account for 30%–50% of all CMT cases (Dubourg et al., 2006).

The CMT type 4 (CMT4) is an autosomal recessive demyelinating form of CMT characterized by an earlier onset of symptoms than autosomal dominant CMT1 (Berciano & Combarros, 2003; Parman & Battaloğlu, 2013). CMT4 is

*Corresponding author: KI W. CHUNG, Department of Biological Science, Kongju National University, 56 Gongjudaehak-ro, Gongju, Chungnam 314–701, Korea. E-mail: kwchung@kongju.ac.kr
†These authors contributed equally to this work.

further divided into many subtypes from CMT4A to CMT4J based on clinical phenotypes and genetic causes. Mutations in more than 10 genes (*GDAP1, MTMR2, SBF1*, *SBF2*, *NDRG1*, *HK1*, *MPZ*, *EGR2*, *SH3TC2*, *PRX*, *FGD4*, *FIG4*, and *SURF1*) have been shown to cause CMT4 (Echaniz-Laguna et al., 2013; Nakhro, Park, Hong et al., 2013; Tazir et al., 2013).

Specifically, CMT type 4H (CMT4H; MIM 609311) is caused by mutations in the *FGD4* gene (MIM 611104) and is characterized by first-decade onset, slow progression, areflexia, and frequent scoliosis (Delague et al., 2007; Stendel et al., 2007). Since CMT4H was first mapped on chromosome 12p11.21-q13.11 by linkage analysis in consanguineous Mediterranean families (De Sandre-Giovannoli et al., 2005), Delague et al. (2007) identified different homozygous mutations p.Met298fs*8 and p.Met298Thr) in the *FGD4* gene from each family. Most CMT4H cases have been reported in the Mediterranean region, whereas they have been rarely reported in other regions. Most CMT4H patients have homozygous mutations in the *FGD4* gene (Delague et al., 2007; Stendel et al., 2007; Fabrizi et al., 2009; Houlden et al., 2009; Baudot et al., 2012; Arai et al., 2013; Boubaker et al. 2013; Zimoń et al., 2015), except for a Japanese case (Hayashi et al., 2013).

FGD4 encodes FRABIN (*F*GD1-*r*elated F-*a*ctin *bin*ding protein), an F-actin binding (FAB) protein, which is a GDP/GTP exchange factor (GEF) for CDC42 and possesses actin filament (F-actin)-binding activity (Ikeda et al., 2001). The function of FRABIN is still not clear in the peripheral nervous system. Mouse FRABIN induces CDC42-mediated cell-shape changes in transfected Schwann cells, suggesting that Rho GTPase signaling plays an important role in the myelination of peripheral axons (Stendel et al., 2007). Expression levels of *FGD4* in mice are lower in postnatal and adult nervous tissue than in embryonic nerves, also suggesting a role *FGD4* in the early stages of the myelination process (Delague et al., 2007).

To assess the frequency and clinical phenotype of CMT4H with *FGD4* pathogenic variants in a Korean CMT cohort, we performed genetic tests of 17p12 (*PMP22*) duplication and exome sequencing in Korean 594 CMT families, and identified two CMT4H families harboring novel compound heterozygous *FGD4* mutations.

Materials and Methods

Patients

We enrolled 594 unrelated CMT families from a Korean CMT cohort study group. Of these, 297 families were determined to have members with the demyelinating type of CMT. For sporadic cases, paternities were determined by genotyping of 15 microsatellites using a PowerPlex 16 System (Promega, Madison, WI, USA). In addition to the CMT families, 300 healthy individuals were examined as controls. Written informed consent was obtained from all participants according to a protocol approved by the Institutional Review Board for Sungkyunkwan University, Samsung Medical Center, and Kongju National University (Industry-Cooperation Foundation).

DNA Preparation and 17p12 Duplication Test

Genomic DNA was purified from peripheral blood using a QIAamp blood DNA purification kit (Qiagen, Hilden, Germany). All patient samples were screened for a 17p12 (*PMP22*) duplication/deletion, which is the primary genetic cause of demyelinating CMT, using hexaplex microsatellite PCR analysis (Choi et al., 2007).

Exome Sequencing and Determination of Causative Mutations

After removal of 17p12 duplication patients, whole exome sequencing or CMT-related gene-targeted sequencing was applied in all remaining patients. Exome sequencing was performed using the Human SeqCap EZ Human Exome Library ver. 3.0 (Roche/NimbleGen, Madison, WI, USA), and the HiSeq 2000 Genome Analyzer (Illumina, San Diego, CA, USA) for affected individuals of the two families (II-3 in FC73, II-1 in FC646) using a previously published method (Choi et al., 2012; Kim et al., 2015). The UCSC assembly hg19 was used as the reference sequence. Variant calls were achieved in those with ≥20 single-nucleotide polymorphism (SNP) quality. Functionally significant variants (missense, nonsense, exonic indel, and splicing site variants) were selected from CMT-associated genes, and these were then checked as to whether they were registered in the dbSNP142 database (http://www.ncbi.nlm.nih.gov), the 1000 Genomes Project (1000G) database (http://www.1000genomes.org/), the Exome Variant Project (EVP) database (http://evs.gs.washington.edu/EVS/), and the Exome Aggregation Consortium (ExAC) database (http://exac.broadinstitute.org/).

Candidate causative variants were confirmed by Sanger sequencing for extended family members using an ABI3130XL genetic analyzer (Applied Biosystems, Foster City, CA, USA). Mutations were considered causative when they: (1) fitted for recessive inheritance or occurred by *de novo* mutation, (2) cosegregated with affected members, (3) were not found in any of the 300 healthy controls,

and (4) were not reported in the dbSNP142 database, the 1000 Genomes Project database, or the EVP. We also considered genotype-phenotype correlation for candidate variants. Genomic evolutionary rate profiling (GERP) scores were determined by the GERP++ program (http://mendel.stanford.edu/SidowLab/downloads/gerp/index.html). *In silico* analyses were performed using the prediction algorithms of SIFT (http://sift.jcvi.org), MUpro (http://www.ics.uci.edu/~baldig/mutation), and PolyPhen2 (http://genetics.bwh.harvard.edu/pph2/).

Clinical and Electrophysiological Assessments

Clinical information was obtained in a standardized manner and included assessments of motor and sensory impairments, deep tendon reflexes, and muscle atrophy. Muscle strength of flexor and extensor muscles was assessed manually using the standard medical research council (MRC) scale. To quantify physical disability, disease severity was determined for each patient using a nine-point functional disability scale (FDS) (Birouk et al., 1997). Sensory impairments were assessed in terms of responses to different levels and severities of pain, temperature, vibrational, and positional stimuli.

Motor and sensory conduction velocities of median, ulnar, peroneal, tibial, and sural nerves were determined. MNCVs of the median and ulnar nerves were determined by stimulating the elbow and wrist, while recording compound muscle action potentials (CMAPs) over the abductor pollicis brevis and adductor digiti quinti, respectively. In the same way, NCVs of peroneal and tibial nerves were determined by stimulating the knee and ankle, while recording CMAPs over the extensor digitorum brevis and adductor hallucis, respectively. Sensory nerve conduction velocities (SNCVs) and sensory nerve action potentials (SNAPs) were obtained over the finger-wrist segment from the median and ulnar nerves by orthodromic scoring and were also recorded for sural nerves.

Magnetic Resonance Imaging (MRI) of Hip, Thigh, and Lower Leg

MRIs were obtained from the hip, thigh, and lower leg, using a 1.5-T system (Siemens Vision, Siemens, Germany). The imaging was prepared by axial (field of view [FOV] = 24–32 cm, slice thickness = 10 mm, and slice gap = 0.5–1.0 mm) and coronal planes (FOV = 38–40 cm, slice thickness = 4–5 mm, slice gap = 0.5–1.0 mm), using the following protocol: T1-weighted spin-echo (SE) (TR/TE 570–650/14–20, 512 matrixes), T2-weighted SE (TR/TE 2800–4000/96–99, 512 matrixes), and fat-suppressed T2-weighted SE (TR/TE 3090–4900/85–99, 512 matrixes).

Distal Sural Nerve Biopsy

Distal sural nerve biopsies were performed in the patient from family FC646 at 20 years old, and in the patient from family FC73 at 31 years old. In addition to light microscopic examination of formalin-fixed sections, electron microscopic observations were made using specimens fixed in 2% glutaraldehyde in 0.025 M cacodylate buffer (pH 7.4) and processed for semithin and ultrathin studies. Semithin sections were stained with toluidine blue for evaluation by light microscope. Ultrathin sections (60–65 nm) were contrasted with uranyl acetate and lead citrate for ultrastructural studies (H-7650, Hitachi, Japan). The density of myelinated fibers (MFs), axonal diameter, myelin thickness, and g-ratio of MFs were determined from semithin transverse sections using a computer-assisted image analyzer (AnalySIS, Soft Imaging System, GmbH, Germany).

Results

Identification of Compound Heterozygous Mutations in FGD4

Exome sequencing analysis identified novel compound heterozygous mutations in the *FGD4* gene in two recessive demyelinating CMT families, FC646 and FC73 (Figs 1A and B), from filtering of the functionally significant variants in more than 70 CMT-related genes. Except for affected probands, no other family member exhibited peripheral neuropathy in either pedigree. The affected individual from the FC646 family showed c.1034T>C (p.Met345Thr) and c.2043+1G>A (splicing donor), and the affected individual in the FC73 family showed c.1403G>A (p.Arg468Gln) and c.1512-2A>G (splicing acceptor). Capillary DNA sequencing confirmed that each parent transferred a mutation to the affected progeny in both families, and no unaffected member showed both mutations (Fig. 2A). The genotype of each mutation is indicated at the bottom of all examined individuals in the pedigree (Fig. 1). Sequencing of the cDNA from patient FC646:II-I showed that when the intron 16 donor splice site is mutated, a cryptic donor splice site in exon 16 is used instead, giving rise to a frame shift and premature termination of the protein: the c.2043+1G>A splice site mutation might consequently be described as p.Trp663Trpfs*30 (Fig. 2B). All identified mutations were absent in the 300 healthy controls, and have not been reported in the dbSNP142, the 1000G, EVP, and ExAC databases, except for c.1403G>A (very low allele frequency of 1/121408 chromosomes in ExAC). Two missense mutations, p.Met345Thr and p.Arg468Gln, were located in the highly conserved RhoGEF and PH domains in the FGD4 protein, respectively (Figs 2C and D). GERP scores for all the

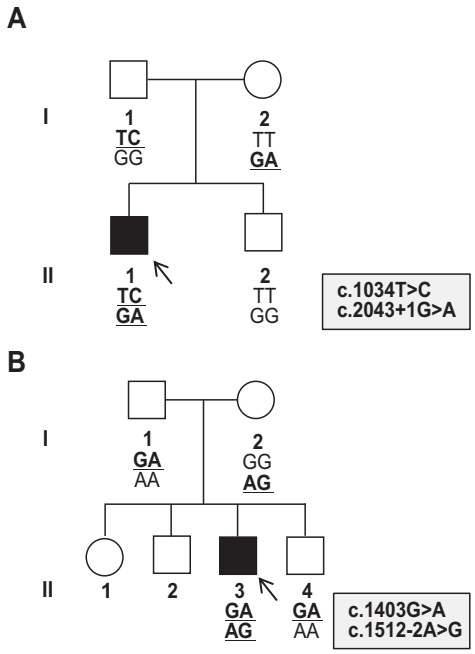

Figure 1 Pedigrees of two Charcot-Marie-Tooth disease type 4H families. Open symbols and filled symbols represent the unaffected and affected individuals, respectively. Arrows indicate the proband in each family. Genotypes of the *FGD4* mutations are indicated at the bottom of all examined individuals (mutant alleles are indicated by bold underlined letters). (A) FC646 family and (B) FC73 family.

mutation sites were high, with values of more than 5, and 3 *in silico* analyses (SIFT, PolyPhen-2, and MUpro) predicted pathogenic effects for the two missense mutations (Table 1). This may arouse suspicion of genetic paternity, because all the parents were unaffected in both families. However, paternities were confirmed by the 15 microsatellite genotyping test.

In addition to the *FGD4* causative mutations, many functionally significant variants were detected in CMT-related genes from two patients. However, these were considered polymorphic or rare private variants, because they were found in controls including several human genome variant databases. Several variants were not found in controls, but they did not cosegregate with the affected individual in each family.

Noncausative Functionally Significant Variants in FGD4

Exome sequencing revealed five more functionally significant *FGD4* variants in Korean CMT cohort (Table 2). The p.Ser68Phe and p.Thr125Met variants were relatively frequent in controls and were reported in several global human genome variant databases. Thus, they were determined to be noncausative polymorphic variants. Other variants (p.Arg583X, p.Tyr362fs, and pGlu528Ala) were not reported yet or very rarely reported, however, none of these fitted the autosomal recessive inheritance mode. Thus, they were not considered as an underlying cause of the CMT. However, we cannot exclude their possible pathogenic impact when they are present in the homozygous state or along with other functionally significant heterozygous partners.

Clinical Manifestations

Patient 1: A 20-year-old man (II-1, Fig. 1A), was born healthy at full term by spontaneous vaginal delivery to healthy nonconsanguineous parents. Neither his parents nor siblings exhibited any motor impairment. He had no history of gestational or perinatal problems, and was able to walk at the age of 1. At age 6, gait disturbance and high-arched feet were noted by his parents. Neurologic examination at age 20 revealed muscle weakness predominantly in the distal portions of the upper and lower limbs. Scoliosis was also observed. Perception of vibration and position was more perturbed than pain and temperature sensation. Deep tendon reflexes were absent in all four limbs and postural instability was observed. He could walk without assistance, but was not able to run (FDS score: 2). Electrophysiological studies demonstrated markedly reduced motor nerve conduction velocities (NCVs); the range of motor NCVs were from 10.1 m/sec to 15.3 m/sec. Median MNCVs were below 13.0 m/sec. SNAPs in median, ulnar, and sural nerves were not elicited (Table 3). Needle electromyography (EMG) was compatible with neuropathy with fibrillation potentials and neurogenic motor unit action potentials.

Patient 2: A 46-year-old man (II-3, Fig. 1B), was born to nonconsanguineous unaffected parents. Early motor milestones were not delayed, but he first noticed weakness in legs and gait disturbance at 8 years of age. On neurologic examination at age 46, we found muscle weakness and atrophy predominantly in the distal portions of his limbs. He presented with proximal muscular weakness in the lower limbs. Vibratory perception was reduced in all limbs, and sensory loss to pain and temperature was observed in the lower limbs. Deep tendon reflexes were absent in all four limbs. Postural instability, pes cavus, and scoliosis were observed. He walked with difficulty, but could still do so unaided (FDS score: 3). We could not observe CMAPs in the median, ulnar, peroneal, and tibial motor nerves. Also, SNAPs in the median, ulnar, and sural nerves were not detected (Table 3). EMG was compatible with chronic neuropathic features.

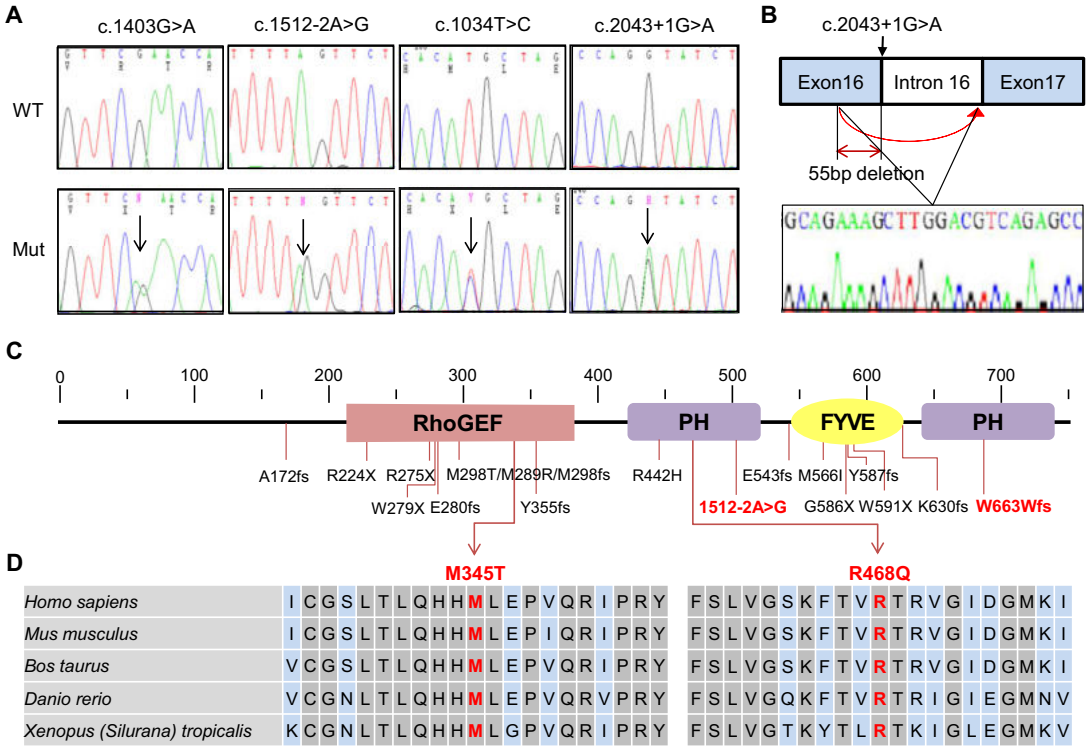

Figure 2 Sequencing chromatograms and conservation analysis for *FGD4* mutations. (A) Sequencing chromatograms of the four mutation sites. Mutation sites are indicated by vertical arrows. (B) Alteration of splicing by the c.2043+1G>A mutation. Sequencing of *FGD4* cDNA revealed an additional deletion of 55-bp on the exon 16. The cDNA was synthesized using the mRNA purified from fibroblast in the patient (FC646, II-1). (C) FGD4 protein structure and causative mutations. The present four mutations as well as previously reported mutations are indicated below the diagram (RhoGEF: guanine nucleotide exchange factor for Rho/Rac/Cdc42-like GTPases, PH: pleckstrin homology, FYVE: Fab 1, YOTB, Vac 1, and EEA1 zinc finger domain). (D) Conservation of amino acid sequences in the mutation sites. Multiple protein sequence alignment revealed strong conservation of amino acid sequences at the p.Met345Thr and p.Arg468Gln mutation sites among different vertebrate species (*Homo sapiens*: NP_640334.2, *Mus musculus*: NP_631978.1, *Bos taurus*: XP_002687755.2, *Danio rerio*: NP_001171404.1, and *Xenopus tropicalis*: XP_002942337.2).

Table 1 GERP scores and *in silico* analysis of pathogenic mutations in *FGD4*.

Program	c.1512-2A>C (Splicing)	c.2043+1G>A (Trp663Trpfs*30)	c.1034T>C (Met345Thr)	c.1403G>A (Arg468Gln)	Prediction
GERP	5.39	5.18	5.47	5.67	Highly conserved
In silico analysis of protein					
SIFT	–	–	0.000[1]	0.010[1]	Affected function
PolyPhen-2	–	–	1.000[1]	1.000[1]	Damaging
MUpro	–	–	−0.781[1]	−0.140[1]	Decreased stability

[1]Indicates prediction of pathogenic.
Abbreviation: GERP, genomic evolutionary rate profiling score.

Mild Fatty Involvements in the Lower Leg Muscles

Lower limb MRIs showed distal predominant fatty infiltration in patient (II-1) of the FC646 family (Figs 3A–D). Hip and thigh MRIs did not show fatty infiltrations (Figs 3B and C). However, MRIs showed predominant fatty infiltrations and muscle atrophy in the bilateral tibialis anterior muscles compared to the soleus, gastrocnemius and peronei muscles at the calf level (Fig. 3D).

Table 2 Observed nonsynonymous heterozygous variants in *FGD4*: considered as nonpathogenic.

Variants		Databases					
Nucleotide	Amino acid	dbSNP142	1000G[1]	ESP[2]	ExAC[3]	Observed family number[4]	Comments
c.203C>T	p.Ser68Phe	Rs544427828	N	N	0.00008	3	Rare pol nonsegregated
c.374C>T	p.Thr125Met	rs200732890	0.0023	0.0002	0.00095	14	Rare pol
c.1747C>T	p.Arg583X	N	N	N	<0.00001	1	Private variant nonsegregated
c.1086_1087insT	p.Tyr362fs	N	N	N	<0.00001	1	Private variant segregated by dominance
c.1583A>C	p.Glu528Ala	N	N	N	N	2	Rare pol nonsegregated

[1]Variant allele frequencies in the 1000 Genome Project database (Nov 2014).
[2]ESP: Variant allele frequencies in the Exome Sequencing Project (Nov 2014).
[3]ExAC: Variant allele frequencies in the Exome Aggregation Consortium Browser (Ver. 0.3).
[4]Generated from 305 exome sequencing data of Korean CMT patients.
Abbreviations: N, unreported, pol, polymorphism.

Table 3 Clinical and electrophysiological features of two Korean CMT4H patients.

Patient	Patient 1 (FC646)	Patient 2 (FC73)
Consanguinity	Nonconsanguineous	Nonconsanguineous
Mutation	c.1034T>C c.2043+1G>A	c.1403G>A c.1512-2A>C
Gender	Male	Male
Age at onset (years)	6	8
Age at exam (years)	20	46
FDS	2	3
Distal weakness		
Upper limb[1]	+	+
Lower limb[2]	+	++
Distal muscle atrophy	Mild	Moderate
Sensory loss	Yes	Yes
Deep tendon reflexes	Absent	Absent
Scoliosis	Yes	Yes
Pes cavus	Yes	Yes
Postural instability	Yes	Yes
Median nerve (right/left)		
CMAP (mV)	14.7/12.5	NP/NP
MNCV (m/s)	12.6/13.0	NP/NP
Peroneal nerve (right/left)		
CMAP (mV)	2.5/2.8	NP/NP
MNCV (m/s)	10.3/11.3	NP/NP
Sural nerve (right/left)		
SNAP	NP/NP	NP/NP
SNCV (m/s)	NP/NP	NP/NP

[1]+Intrinsic hand weakness 4/5 on the MRC scale.
[2]+Ankle dorsiflexion 4/5 on MRC scale.
[b]++Ankle dorsiflexion <4/5 on the MRC scale.
Abbreviations: FDS, functional disability scale; NP, no potential; CMAP, compound muscle action potential; MNCV, motor nerve conduction velocity; SNAP, sensory nerve action potential; SNCV, sensory nerve conduction velocity.

Sural Nerve Biopsy

In both patients, pathological findings of the distal sural nerve biopsies revealed similar chronic demyelinating neuropathy. Unfortunately, patient 2 had undergone sural nerve biopsy in another university hospital 15 years ago; thus, only the pathology results records remained. However, in patient 1, sural nerve biopsy was performed last year and a full evaluation was carried out. Semithin transverse sections in patient 1 (II-1, Fig. 1A) showed absence of large MFs, leaving

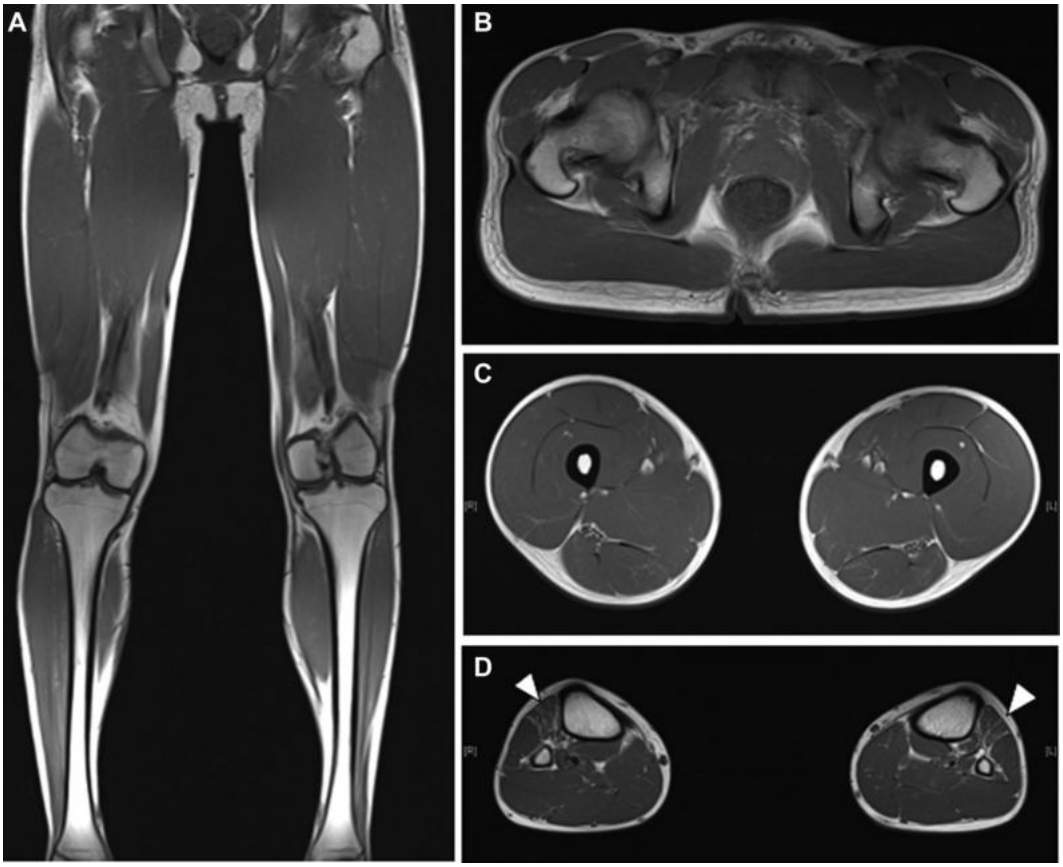

Figure 3 Hip, thigh, and lower leg MRIs from a CMT4H patient. T1-weighted coronal (A) and axial MRIs (B–D) were obtained from patient 1. (A–C) No muscular atrophy or fatty infiltration was observed at the hip or thigh levels. (D) However, the calf-level image revealed fatty infiltration in the bilateral tibialis anterior muscle (arrowheads) compared to peroneal and soleus muscles.

medium and small MFs and scattered MFs with focally folded myelin as well as suggestive onion bulb formations (Fig. 4A). The remaining MF count was 6083/mm^2 (normal distal sural nerve in 21-year-old male: 10,000/mm^2). The range and average diameter of MFs were 0.99–6.26 μm and 2.67 μm, respectively (range and average diameter of MFs in normal distal sural nerve of 21-year-old males: 2.2–14.2 μm and 5.4 μm, respectively). Histogram analysis showed a unimodal distribution pattern with MF diameter less than 3 and 6 μm constituting 65.9% and 99.6% of MFs, respectively (Fig. 4B). The MF% area in this case was 3.8% (normal sural nerve of 21-year-old male: 36.5%). The range and average g-ratio (axonal diameter/MF diameter) were 0.46–0.87 and 0.69 $\pm$ 0.08, respectively (mean g-ratio in age 21–50 years: 0.66). A g-ratio of more than 0.7 (abnormally thin myelin sheath) made up 47.6% of all MFs examined, and no MFs possessed a g-ratio less than 0.4 (abnormally thick myelin sheath). Electron microscopic examination revealed scattered myelinated axons with severely folded myelin or focally folded myelin, as well as occasionally noted uncompacted myelin sheaths (Fig. 4C). Onion bulbs containing hypomyelinated axons were also noted frequently (Fig. 4D).

Discussion

In this study, we identified two different pairs of novel compound heterozygous mutations in the *FGD4* gene from non-consanguineous Korean CMT4H families (p.Arg468Gln and c.1512-2A>C in FC73, p.Met345Thr and p.Trp663Trpfs*30 in FC646). No other family members exhibited any kind of peripheral neuropathy. This is the first report of Korean CMT4H cases. In Asia, several Japanese patients have been recently reported as CMT4H cases, with homozygous or compound heterozygous mutations (Arai et al., 2013; Hayashi et al., 2013). We believe that these mutations are the underlying causes of the CMT4H phenotype in both families, because they cosegregated with affected members in an autosomal

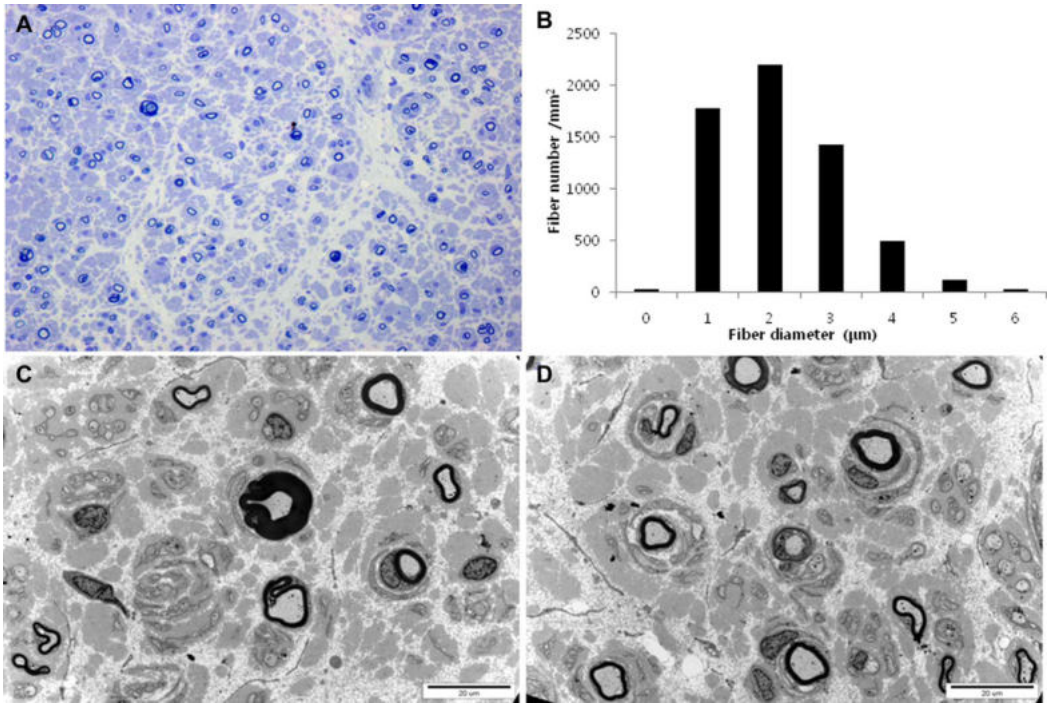

Figure 4 Histopathological characterization of the distal sural nerve biopsy from the patient 1. (A) Semithin transverse section. It revealed almost complete loss of large myelinated fibers (MFs) with remaining medium- and small-sized MFs (toluidine blue-stained semithin transverse section, original magnification ×400). (B) Histogram of unimodal MF distribution pattern. (C) Electron micrographs from transverse sections of sural nerve revealed scattered myelinated axons with excessively folded myelin or focally folded myelin. In addition, occasional decompaction of myelin sheaths was observed (original magnification ×3000). (D) Onion bulbs containing hypomyelinated axons were also noted (original magnification ×3000).

recessive manner, but were not found in controls (n = 300) or any of the major global human genome variation databases (dbSNP142, 1000G, EVS, and ExAC databases). Additionally, two missense alleles were located in the well-conserved RhoGEF (p.Met345Thr) and PH (p.Arg468Gln) domains, and *in silico* analyses predicted these to be pathogenic. In particular, modeling analysis supported the theory that Rho GTPase signaling and regulation of Cdc42 by Frabin/*FGD4* in Schwann cells play an important role in the structure and function of the peripheral nervous system (Stendel et al., 2007; Horn et al., 2012). Exome sequencing also indicated no other variant as the underlying cause.

CMT4H was first reported to be a novel locus on chromosome 12p11.21-q13.11 by De Sandre-Giovannoli et al. (2005). Subsequently, Delague et al. (2007) identified homozygous mutations in the *FGD4* gene. To date, more than 15 mutations have been reported to be the underlying causes of CMT4H (Delague et al., 2007; Stendel et al., 2007; Fabrizi et al., 2009; Houlden et al., 2009; Baudot et al., 2012; Arai et al., 2013; Boubaker et al., 2013; Hayashi et al., 2013; Zimoń et al., 2015). Mutations are located most abundantly in the RhoGEF domain (p.Arg224X, p.Arg275X, p.Trp279X, p.Glu280fs, p.Met298fs, p.Met298Thr, and p.Tyr355fs), followed by the FYVE (p.Glu543fs, p.Met566Ile, p.Gly586X, p.Tyr587fs, p.Trp591X, and Lys630fs) and PH domain (p.Arg442His). In this study, one mutation (p.Met345Thr) was located in the RhoGEF domain, and three were in the PH domain (p.Arg468Gln, p.Trp663Trpfs, and c.1512-2A>C). As in our cases, splicing mutations have also been reported several times (Delague et al., 2007; Stendel et al., 2007; Fabrizi et al., 2009; Arai et al., 2013; Hayashi et al., 2013).

All documented mutations have been reported from consanguineous (major) or nonconsanguineous (minor) families. CMT4H patients with homozygous *FGD4* gene mutations are characterized by early onset of symptoms, slow disease progression, areflexia, myelin outfolding, and frequent scoliosis (Delague et al., 2007; Stendel et al., 2007). Both patients with compound heterozygous *FGD4* mutations showed similar clinical phenotypes of CMT4H patients with homozygous mutations. Following 14 years progression, lower limb MRI in patient 1 revealed only mild fatty replacements in the bilateral tibialis anterior muscles, while hip and thigh

muscles were normal. These findings support the hypothesis that although symptoms of CMT4H appeared within the first decade of life, the disease progression was very slow. In addition, MRIs also showed length-dependent neuronal degeneration in CMT4H.

This study identified two CMT4H cases from 594 Korean CMT families with a frequency of 0.003 (0.007 in demyelinating cases), suggesting that CMT4H occurrence is rare in the East Asian population. To our knowledge, these are the first cases of CMT4H of Korean origin, and this study provided further evidence that compound heterozygous mutations in *FGD4* cause CMT4H. Thus, *FGD4* assay could be considered as a means to screen slow progressive demyelinating CMT patients from nonconsanguineous families.

Acknowledgment

This study was supported by the Korean Health Technology R&D Project, Ministry of Health and Welfare (A120182) and by the National Research Foundation (NRF) grants funded by the Korean government, MSIP (2014R1A2A2A01003164 and 2014R1A2A2A01004240).

References

Arai, H., Hayashi, M., Hayasaka, K., Kanda, T. & Tanabe, Y. (2013) The first Japanese case of Charcot-Marie-Tooth disease type 4H with a novel *FGD4* c.837-1G>A mutation. *Neuromuscul Disord* **23**, 652–655.

Baudot, C., Esteve, C., Castro, C., Poitelon, Y., Mas, C., Hamadouche, T., El-Rajab, M., Lévy, N., Megarbané, A. & Delague, V. (2012) Two novel missense mutations in FGD4/FRABIN cause Charcot-Marie-Tooth type 4H (CMT4H). *J Peripher Nerv Syst* **17**, 141–146.

Berciano, J. & Combarros, O. (2003) Hereditary neuropathies. *Curr Opin Neurol* **16**, 613–622.

Birouk, N., Gouider, R., Le Guern, E., Gugenheim, M., Tardieu, S., Maisonobe, T., Le Forestier, N., Agid, Y., Brice, A. & Bouche, P. (1997) Charcot-Marie-Tooth disease type 1A with 17p11.2 duplication. Clinical and electrophysiological phenotype study and factors influencing disease severity in 119 cases. *Brain* **120**, 813–823.

Boubaker, C., Hsairi-Guidara, I., Castro, C., Ayadi, I., Boyer, A., Kerkeni, E., Courageot, J., Abid, I., Bernard, R., Bonello-Palot, N., Kamoun, F., Cheikh, H. B., Lévy N., Triki, C. & Delague, V. (2013) A novel mutation in FGD4/FRABIN causes Charcot-Marie-Tooth disease type 4H in patients from a consanguineous Tunisian family. *Ann Hum Genet* **77**, 336–343.

Choi, B. O., Kim, J., Lee, K. L., Yu, J. S., Hwang, J. H. & Chung, K. W. (2007) Rapid diagnosis of CMT1A duplication and HNPP deletions by multiplex microsatellite PCR. *Mol Cells* **23**, 39–48.

Choi, B. O., Koo, S. K., Park, M. H., Rhee, H., Yang, S. J., Choi, K. G., Jung, S. C., Kim, H. S., Hyun, Y. S., Nakhro, K., Lee, H. J., Woo, H. M. & Chung, K. W. (2012) Exome sequencing is an efficient tool for genetic screening of Charcot-Marie-Tooth disease. *Hum Mutat* **33**, 1610–1615.

Delague, V., Jacquier, A., Hamadouche, T., Poitelon, Y., Baudot, C., Boccaccio, I., Chouery, E., Chaouch, M., Kassouri, N., Jabbour, R., Grid, D., Mégarbané, A., Haase, G. & Lévy, N. (2007) Mutations in *FGD4* encoding the Rho GDP/GTP exchange factor frabin cause autosomal recessive Charcot-Marie-Tooth type 4H. *Am J Hum Genet* **81**, 1–16.

De Sandre-Giovannoli, A., Delague, V., Hamadouche, T., Chaouch, M., Krahn, M., Boccaccio, I., Maisonobe, T., Chouery, E., Jabbour, R., Atweh, S., Grid, D, Mégarbané, A. & Lévy, N. (2005) Homozygosity mapping of autosomal recessive demyelinating Charcot-Marie-Tooth neuropathy (CMT4H) to a novel locus on chromosome 12p11.21-q13.11. *J Med Genet* **42**, 260–265.

Dubourg, O., Azzedine, H., Verny, C., Durosier, G., Birouk, N., Gouider, R., Salih, M., Bouhouche, A., Thiam, A., Grid, D., Mayer, M., Ruberg, M., Tazir, M., Brice, A. & Le Guern, E. (2006) Autosomal-recessive forms of demyelinating Charcot-Marie-Tooth disease. *Neuromolecular Med* **8**, 75–86.

Echaniz-Laguna, A., Ghezzi, D., Chassagne, M., Mayençon, M., Padet, S., Melchionda, L., Rouvet, I., Lannes, B., Bozon, D., Latour, P., Zeviani, M. & Mousson de Camaret, B. (2013) SURF1 deficiency causes demyelinating Charcot-Marie-Tooth disease. *Neurology* **81**, 1523–1530.

Fabrizi, G. M., Taioli, F., Cavallaro, T., Ferrari, S., Bertolasi, L., Casarotto, M., Rizzuto, N., Deconinck, T., Timmerman, V. & De Jonghe, P. (2009) Further evidence that mutations in *FGD4*/frabin cause Charcot-Marie-Tooth disease type 4H. *Neurology* **72**, 1160–1164.

Harding, A. E. & Thomas, P. K. (1980) Hereditary distal spinal muscular atrophy. A report on 34 cases and a review of the literature. *J Neurol Sci* **45**, 337–348.

Hayashi, M., Abe, A., Murakami, T., Yamao, S., Arai, H., Hattori, H., Iai, M., Watanabe, K., Oka, N., Chida, K., Kishikawa, Y. & Hayasaka, K. (2013) Molecular analysis of the genes causing recessive demyelinating Charcot-Marie-Tooth disease in Japan. *J Hum Genet* **58**, 273–278.

Horn, M., Baumann, R., Pereira, J. A., Sidiropoulos, P. N., Somandin, C., Welzl, H., Stendel, C., Lühmann, T., Wessig, C., Toyka, K. V., Relvas, J. B., Senderek, J. & Suter, U. (2012) Myelin is dependent on the Charcot-Marie-Tooth type 4H disease culprit protein FRABIN/FGD4 in Schwann cells. *Brain* **135**, 3567–3583.

Houlden, H., Hammans, S., Katifi, H. & Reilly, M. M. (2009) A novel frabin (FGD4) nonsense mutation p.R275X associated with phenotypic variability in CMT4H. *Neurology* **72**, 617–620.

Ikeda, W., Nakanishi, H., Tanaka, Y., Tachibana, K. & Takai, Y. (2001) Cooperation of Cdc42 small G protein-activating and actin filament-binding activities of frabin in microspike formation. *Oncogene* **20**, 3457–3463.

Kim, H. J., Lee, J., Hong, Y. B., Kim, Y. J., Lee, J. H., Nam, S. H., Choi, B. O. & Chung K. W. (2015) Ser135Phe mutation in HSPB1 (HSP27) from Charcot-Marie-Tooth disease type 2F families. *Genes Genom* **37**, 295–303.

Kleopa, K. A., Georgiou, D.-M., Nicolaou, P., Koutsou, P., Papathanasiou, E., Kyriakides, T. & Christodoulou, K. (2004) A novel PMP22 mutation Ser22Phe in a family with hereditary neuropathy with liability to pressure palsies and CMT1A phenotypes. *Neurogenetics* **5**, 171–175.

Nakhro, K., Park, J. M., Choi, B. O. & Chung, K.W. (2013) Missense mutations in MFN2: polymorphic or incomplete penetration? *Anim Cells Syst* **17**, 228–236.

Nakhro, K., Park, J. M., Hong, Y. B., Park, J. H., Nam, S. H., Yoon, B. R., Yoo, J. H., Koo, H., Jung, S. C., Kim, H. L., Kim, J. Y., Choi, K. G., Choi, B. O. & Chung, K. W. (2013) SET binding factor 1 (SBF1) mutation causes Charcot-Marie-Tooth disease type 4B3. *Neurology* **81**, 165–173.

Pareyson, D. & Marchesi, C. (2009) Diagnosis, natural history, and management of Charcot-Marie-Tooth disease. *Lancet Neurol* **8**, 654–667.

Parman, Y. & Battaloğlu, E. (2013) Recessively transmitted predominantly motor neuropathies. *Handb Clin Neurol* **115**, 847–861.

Rossor, A. M., Polke, J. M., Houlden, H. & Reilly, M. M. (2013) Clinical implications of genetic advances in Charcot-Marie-Tooth disease. *Nat Rev Neurol* **9**, 562–571.

Stendel, C., Roos, A., Deconinck, T., Pereira, J., Castagner, F., Niemann, A., Kirschner, J., Korinthenberg, R., Ketelsen, U.-P., Battaloglu, E., Parman, Y., Nicholson, G., Ouvrier, R., Seeger, J., De Jonghe, P., Weis, J., Krüttgen, A., Rudnik-Schöneborn, S., Bergmann, C., Suter, U., Zerres, K., Timmerman, V., Relvas, J. B. & Senderek, J. (2007) Peripheral nerve demyelination caused by a mutant Rho GTPase guanine nucleotide exchange factor, Frabin/*FGD4*. *Am J Hum Genet* **81**, 158–164.

Tazir, M., Bellatache, M., Nouioua, S. & Vallat, J. M. (2013) Autosomal recessive Charcot-Marie-Tooth disease: from genes to phenotypes. *J Peripher Nerv Syst* **18**, 113–129.

Zimoń, M., Battaloğlu, E., Parman, Y., Erdem, S., Baets, J., De Vriendt, E., Atkinson, D., Almeida-Souza, L., Deconinck, T., Ozes, B., Goossens, D., Cirak, S., Van Damme, P., Shboul, M., Voit, T., Van Maldergem, L., Dan, B., El-Khateeb, M. S., Guergueltcheva, V., Lopez-Laso, E., Goemans, N., Masri, A., Züchner, S., Timmerman, V., Topaloğlu, H., De Jonghe, P. & Jordanova A. (2015) Unraveling the genetic landscape of autosomal recessive Charcot-Marie-Tooth neuropathies using a homozygosity mapping approach. *Neurogenetics* **16**, 33–42.

Received: 8 January 2015
Accepted: 3 July 2015